

Impact of electrolyser dynamics and high-resolution solar variability on the optimal design and economic profitability of renewable hydrogen systems

Panagis Antzoulatos^a, Nikolaos Skordoulis^b, Konstantinos Braimakis^c

^a *Laboratory of Refrigeration, Air-Conditioning and Solar Energy, School of Mechanical Engineering, National Technical University of Athens (NTUA), Athens, Greece, mc21005@mail.ntua.gr, CA*

^b *Laboratory of Thermal Processes, Thermal Engineering Section, School of Mechanical Engineering, National Technical University of Athens (NTUA), Athens, Greece, nskordoulis@mail.ntua.gr*

^c *Laboratory of Refrigeration, Air-Conditioning and Solar Energy, School of Mechanical Engineering, National Technical University of Athens (NTUA), Athens, Greece, mpraim@central.ntua.gr*

Abstract:

Renewable hydrogen produced via water electrolysis powered by renewable energy sources (RES) is a key pathway for decarbonizing sectors where direct electrification remains challenging, such as heavy industry and long-distance transport. Under the latest EU framework, direct coupling of electrolysers with intermittent RES, particularly solar photovoltaics, is a straightforward approach to ensuring renewable hydrogen production. However, most existing studies rely on hourly-resolution data and simplified electrolyser models, neglecting short-term variability, partial-load efficiency, and transient operation. In this work, a detailed dynamic electrolyser model is developed, incorporating partial-load efficiency, operational constraints, multiple operating states (on, standby, off), and realistic transition dynamics. Historical solar generation data are downscaled to a 30-minute resolution to capture intra-hour variability. The optimal solar-to-electrolyser capacity ratio is determined by minimizing the Levelised Cost of Hydrogen (LCOH). Results show that undersizing the PV system leads to poor electrolyser utilization and high costs, while excessive oversizing results in limited hydrogen gains and significant energy curtailment. For Greece, using TRIERES electrolyser data, the optimal design is achieved at a capacity ratio of $r = 1.67$, corresponding to an LCOH of 8.18 €/kgH₂. Climatic conditions significantly influence system performance, as the LCOH is reduced for lower solar capacity factors. Overall, the proposed high-fidelity, dimensionless methodology provides a robust framework for optimal sizing and techno-economic assessment of off-grid solar–electrolyser systems.

Keywords:

Alkaline electrolysis; Dynamic simulations; Hydrogen; Intra-minute variations; Levelised Cost of Hydrogen.

1. Introduction

Renewable hydrogen produced via water electrolysis powered by renewable energy sources (RES) is a key pathway for decarbonizing sectors where direct electrification remains challenging, such as heavy industry and long-distance transport[1,2]. Under the latest EU delegated act[3,4], the most straightforward approach to ensuring the renewable character of hydrogen production is the direct coupling of electrolysers with intermittent RES, notably solar photovoltaics and wind energy. While the optimal sizing and techno-economic performance of directly coupled solar–electrolyser systems have been widely examined in the literature[5–8], most existing studies rely on hourly-resolution data[5–8] and simplified electrolyser representations, thereby neglecting short-term renewable generation variability, partial-load efficiency, and transient operating behaviour impact in the optimal sizing and technoeconomic assessment of off-grid solar-electrolyser systems. For off-grid cases, electrolysers work more dynamically than for on-grid applications, and thus, the dynamic operational properties are even more important for economic evaluation.

This study develops a detailed dynamic model of an alkaline electrolyser that incorporates partial-load efficiency behaviour, operational safety constraints, multiple operating states (on, standby, and off), and realistic state transition dynamics (hot start and cold start). To enhance simulation accuracy, historical solar

generation data are downscaled to a 30-minute temporal resolution, allowing for the explicit representation of intra-hour variability. The optimal solar-to-electrolyser capacity ratio is evaluated with the objective of minimizing the Levelised Cost of Hydrogen (LCOH), across different regions to capture the impact of climatic conditions, such as solar irradiation and capacity factor, on both electrolyser performance and hydrogen production cost. The proposed methodology utilizes realistic operational electrolyser models, is dimensionless and applicable to any off-grid solar–electrolyser system, enabling optimal renewable energy sizing and LCOH assessment while incorporating high-fidelity simulations that capture intra-minute variations in renewable power generation.

2. Methodology

2.1. Model overview

The objective of the model is parametric investigation and optimization of the design of off-grid green hydrogen production units that draw power directly from photovoltaic (PV) systems. Specifically, the ratio of nominal PV power to electrolysis nominal power, which leads to the minimization of the LCOH, is determined. The study focuses on the economic viability of hydrogen production, rather than on meeting a specific hydrogen demand profile. For this reason, the existence of storage tanks for the produced hydrogen is not considered, as their size (and thus their cost) depends directly on the demand profile. The system under study is schematically represented in **Figure 1**:

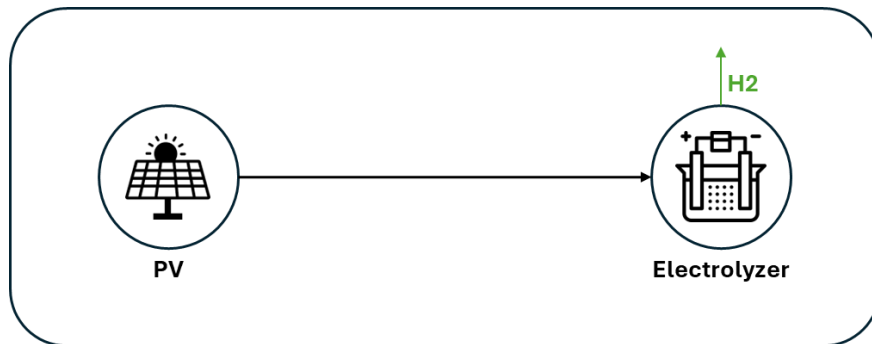


Figure 1: Schematic depiction of the system

The model uses certain technical and economic characteristics of the electrolysis and PV system, as well as the hourly time series of power generation from the PV system as input data. As shown in **Figure 2**, this data is utilized for the annual simulation of the system’s operation, which considers both the behavior of the electrolyser under partial load and the duration of transient operational states during startup. The detailed representation of the plant’s dynamic behavior leads to more accurate results. The simulation’s time resolution is also a model parameter, with its reduction resulting in higher accuracy but also higher computational cost.

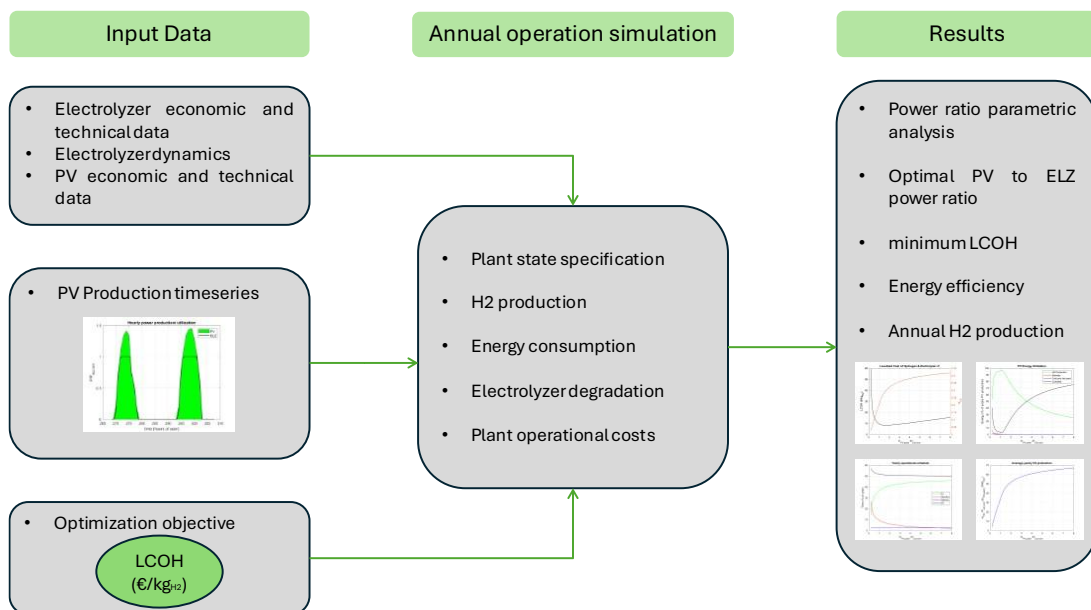


Figure 2: Technoeconomic assessment model overview

Throughout the simulation, the operational state of the system is determined, as well as the hydrogen production, the energy consumption and the degradation of the electrolyser in each time step. In addition, costs related to the electrolysis water consumption are calculated.

This process is iterated automatically for various nominal power ratios, r , between the PV system and the electrolyser. Power ratio r is defined as follows:

$$r = \frac{P_{PV,nom}}{P_{ELz,nom}} \quad (1)$$

The results obtained pertain to the variation of LCOH as a function of r , as well as other performance indicators of the unit, such as the average annual hydrogen production, the renewable energy utilization factor and the electrolyser's capacity factor. Finally, an investigation is conducted into the effect of local climatic conditions on the facility's performance. This is essential for a comprehensive techno-economic evaluation of the system, given the nature of renewable energy, which is characterized by high variability and low predictability.

2.2. Annual operation simulation

2.2.1. Plant state determination

The identification of the system's state of operation at each time step is essential for the calculation of the amount of hydrogen produced and the electrolyser's energy consumption. The logic of the possible states and transitions, as well as the required power and time for each transition, is illustrated in **Figure 3**. The possible states of the system are off, standby, and on. When the power generated by the photovoltaics (P_{PV}) is lower than a specific threshold ($P_{PV} < P_{elz, sb}$), the state of the unit is off, without any energy consumption and hydrogen production. When the power supplied by the photovoltaics is higher than the electrolyser's minimum operating threshold ($P_{PV} \geq P_{ELz, min}$), the electrolyser's state of operation is on and hydrogen is produced according to the system's partial-load performance curve. The standby state is an intermediate state between on and off, during which a small amount of power ($P_{elz} = P_{elz, sb}$) is consumed to maintain operating conditions, but the supplied power is insufficient for hydrogen production.

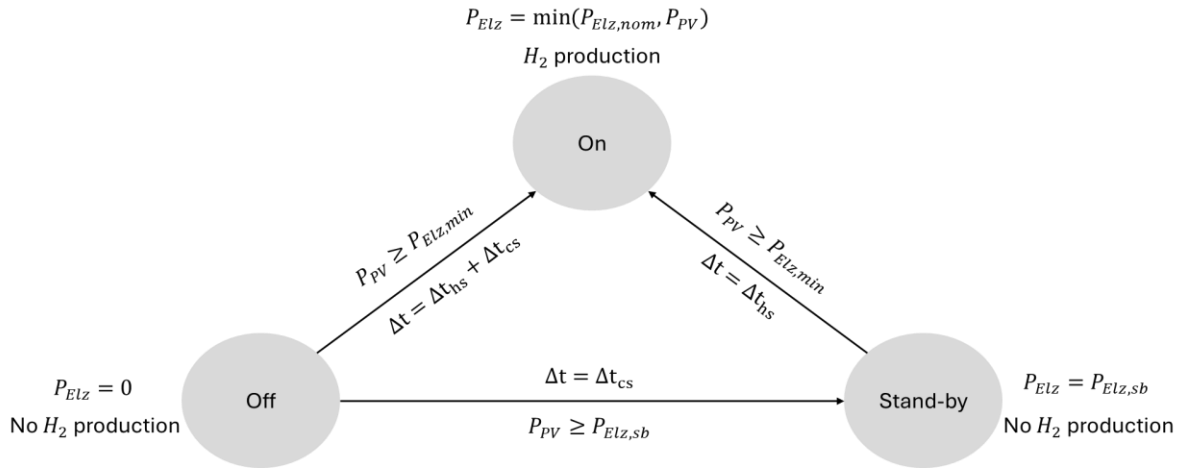


Figure 3: Electrolyser states and transitions

The transition from standby to on (hot start) is significantly faster than the transition from off to on (cold start), as the increase in the electrolyser's temperature and pressure from ambient conditions to operating conditions (70 °C – 90 °C, <30 bar for alkaline electrolysis[1]) requires a notable amount of time. According to various studies, the duration of a cold start can be as long as 50 minutes[1], while a hot start requires only a few minutes[9]. In the present model, the time required for the hot start procedures was set to $\Delta t_{hs} = 3 \text{ min}$. Similarly, the time required to reach operating conditions was set to $\Delta t_{cs} = 30 \text{ min}$. The time required for the cold start was assumed to be the sum of the two time intervals mentioned above. In reality, the latter assumption is rather conservative, because during the cold start, a part of the processes that occur during the hot start happen simultaneously with the heating of the electrolyser and not necessarily in sequence. Hence, the duration of the cold start is expected to be shorter. Finally, the duration of the transition from off to standby is set to Δt_{cs} , as during this transition the electrolyser is heated without any other production startup process.

Consequently, the electrolyser's state of operation at time step j is described by the values of the following variables: $off_j, on_j, sb_j, cs_j, hs_j$. The first three represent the respective states (off, on, standby), while hs_j corresponds to the hot start procedure. cs_j corresponds to the electrolyser heating process. Their value ranges from 0 to 1 and corresponds to the percentage of the time step during which the unit is in the respective state.

For example, suppose that the simulation time step is 30 minutes, and that during the previous time step the unit was in standby mode ($sb_{j-1} = 1$). If the PV output during the current time step (time step j) falls below the threshold required to keep the unit in standby ($P_{PV,j} < P_{Elz,sb}$), then the unit will inevitably switch to the off state with $off_j = 1$. If the generated power is sufficient to maintain operating conditions but is lower than the minimum threshold for hydrogen generation ($P_{Elz,sb} \leq P_{PV,j} < P_{Elz,min}$), then the unit will remain in standby mode, so $sb_j = 1$. Finally, if the PV power is at least equal to the minimum hydrogen production threshold ($P_{PV,j} \geq P_{Elz,min}$), then a hot start is performed to transition the unit from standby to on. Since the duration of the hot start (3 min) is shorter than that of the time step (30 min), the transition is completed before the timestep ends. Thus, $hs_j = \Delta t_{hs} / \Delta t_{ts} = 3 \text{ min} / 30 \text{ min} = 0.1$, where Δt_{ts} is the simulation time step. For the remainder of the time step, the unit's state will be on, so $on_j = (30 \text{ min} - 3 \text{ min}) / 30 \text{ min} = 0.9$. Obviously, for every time step j , the following condition must be satisfied:

$$off_j + sb_j + on_j + hs_j + cs_j = 1. \quad (2)$$

It is noted that the power output of the PV panels is assumed to be constant during each time step as it is based on the historical data used as input time series for the dynamic simulations. Furthermore, transitions from on to off, from on to standby, and from standby to off are assumed to be instantaneous.

2.1.2. Electrolyser energy consumption, H_2 production and operation – related costs

Next, the energy consumption of the electrolyser and the amount of hydrogen produced are calculated. The energy which is consumed at each state of operation at time step j , is determined as follows:

$$E_{elz,on_j} = \min(P_{PV,j}, P_{Elz,nom}) \cdot on_j \cdot \Delta t_{ts}, \quad (3)$$

$$E_{Elz,sb_j} = P_{Elz,sb} \cdot sb_j \cdot \Delta t_{ts}, \quad (4)$$

$$E_{Elz,hs_j} = \frac{P_{Elz,sb} + P_{Elz,min}}{2} \cdot hs_j \cdot \Delta t_{ts}, \quad (5)$$

$$E_{Elz,cs_j} = P_{Elz,sb} \cdot cs_j \cdot \Delta t_{ts}. \quad (6)$$

When the plant remains in off state, energy consumption is zero. During the hot start procedure, the electrolyser power consumption increases from the power consumption of the standby state to the minimum required power for hydrogen production. For this reason, the average power consumed during hot start is assumed to be the mean of the aforementioned values. Thus, the curtailed energy at time step j is calculated as follows:

$$E_{curt_j} = E_{PV_j} - (E_{Elz,on_j} + E_{Elz,sb_j} + E_{Elz,hs_j} + E_{Elz,cs_j}). \quad (7)$$

The mass of the hydrogen produced during timestep j is calculated through the following equation:

$$m_{H2_j} = \eta_{Elz} \cdot E_{Elz,on_j} \cdot \left(1 - \sum_{k=1}^{j-1} (on_k \cdot \Delta t_{ts}) \cdot degr_h\right). \quad (8)$$

In this equation, η_{Elz} is the efficiency of the electrolyser and refers to the mass of hydrogen produced per unit of energy input (kgH₂/kWh). The efficiency is not constant, but it depends on the load of the electrolyser. The last term of the product corresponds to the drop in electrolyser efficiency due to degradation, where $degr_h$ is the percentage drop in electrolyser efficiency per hour of operation.

The operating costs of the facility, which are directly related to its operating schedule, consist of the cost of deionized water for electrolysis and the cost of cooling water. Typically, the volumetric flow rate of the cooling water is known when the electrolyser is operating at its rated load, as well as its cost per volume unit. Assuming that the flow rate is proportional to the load, the cost of the cooling water during timestep j will be:

$$cwc_j = \dot{V}_{CW,nom} \cdot C_{CW} \cdot \frac{\min(P_{PV,j}, P_{Elz,nom})}{P_{Elz,nom}} \cdot \eta_j \cdot \Delta t_{ts}. \quad (9)$$

The deionized water cost at timestep j depends on the amount of hydrogen produced, the required mass of water per mass unit of hydrogen produced (w_{DW}), and the specific cost of water for electrolysis (C_{DW}):

$$dwc_j = m_{H2,j} \cdot w_{DW} \cdot C_{DW}. \quad (10)$$

2.3. Technoeconomic assessment

The results obtained from the annual operational simulation are utilized for the techno-economic evaluation of the system, which includes the calculation of various performance indicators of the facility, particularly the LCOH, the minimization of which is the primary objective of the model. The annual hydrogen production (M_{H2}) is derived from the sum of the individual quantities across all time steps:

$$M_{H2} = \sum_{j=1}^{j^{max}} m_{H2,j}, \quad (11)$$

The annual values for all parameters determined at each simulation time step are calculated in the same way. Other important performance indicators of the facility include the renewable energy utilization factor and the electrolyser's capacity factor:

$$U_{PV} = 1 - E_{curt,a}/E_{PV,a}, \quad (12)$$

$$c_{F,Elz} = E_{Elz,a}/E_{PV,a}. \quad (13)$$

Although the aforementioned indicators do not directly concern the economic viability of the installation, they provide important information regarding the quality of the design in terms of utilizing the capacity of the individual subsystems (PV, electrolyser). For instance, a high value of U_{PV} (e.g., 90%) but a low value of $c_{F,Elz}$ (e.g., 7%) means that, while most of the renewable energy is utilized, the electrolyser receives significantly less energy than it can handle for hydrogen production, resulting in very low output relative to its size. In this way, differences in economic performance observed across different design configurations can be explained.

The LCOH is calculated through the following equation:

$$LCOH = \frac{CAPEX + \sum_{y=1}^L \frac{OPEX_y}{(1+i)^y} + \frac{REPEX}{(1+i)^{LY}}}{\sum_{y=1}^L \frac{M_{H2,y}}{(1+i)^y}} \quad (14)$$

$M_{H2,y}$ is the annual amount of hydrogen produced in year y , considering both the decline in efficiency and any replacement of the electrolyser equipment. The total CAPEX of the facility covers the cost of the PV system and the electrolyser, while OPEX covers operating costs, which consist of maintenance and personnel costs, and the cost of water consumed by the electrolyser. Finally, equipment replacement costs refer to the refurbishment of the electrolyser stacks.

2.4. Input data

The input data for the model were obtained from an actual green hydrogen production plant that is going to be installed at the Motor Oil Hellas refinery in Corinth, as part of the TRIERES hydrogen valley project. Its technical specifications are summarized in **Table 1**.

Table 1. Electrolyser technical data

Parameter	Units	Alkaline electrolyser
Nominal installed capacity	MW	30
Power consumption at standby state	MW	0.3
Degradation	%/1000 h	0.1
Minimum turndown ratio at system level	% (of nominal power)	13.33
Electrolysis water consumption	kg_{H2O}/kg_{H2}	11.11
Cooling water consumption at nominal capacity	m^3/h	840
Stack lifetime	h	80,000

The dependence of the electrolyser's energy consumption on its load, at the beginning of the stacks' life cycle, is shown in **Figure 4**. The efficiency of the electrolyser is defined as the reciprocal of its energy consumption.

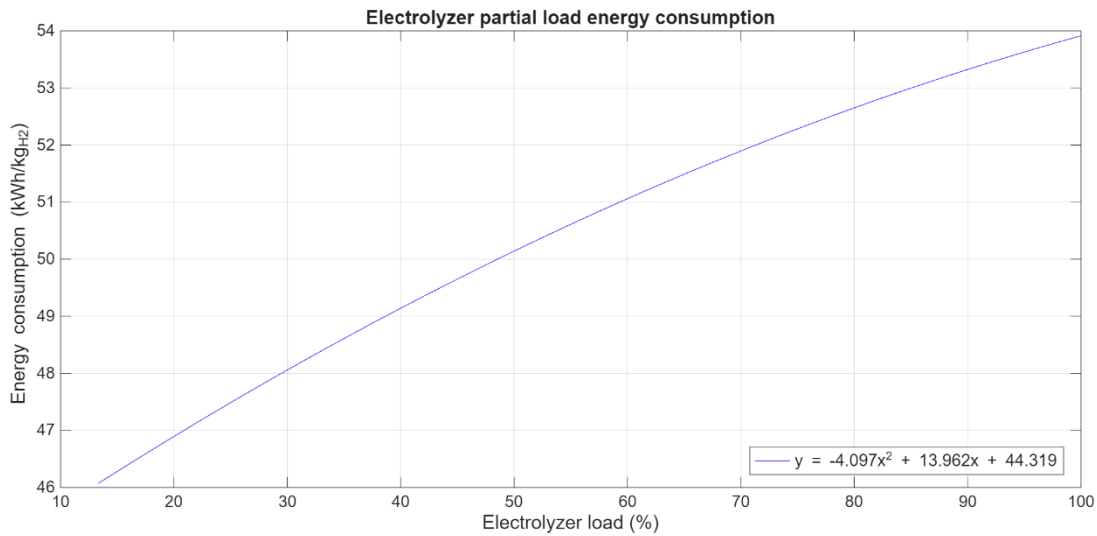


Figure 4: Electrolyzer partial load energy consumption

Finally, the economic data of the system are encapsulated in **Table 2**.

Table 2. System economic data

Parameter	Units	Electrolyser	Photovoltaics
Specific CAPEX	€/kW	1646	700
Specific OPEX	€/kW/year	27.33	15.00
Stack refurbishment cost	€/kW	76	-
Electrolysis water cost	€/m ³	0.7	-
Cooling water cost	€/m ³	0.06	-
Land leasing cost	€/kW/year	-	2.80

The data above were utilized in a similar study [10] that referred to the same electrolysis system, with the main difference being that the electrolyser was assumed to be connected to the power grid. Accordingly, the discount rate is assumed to be $i = 10\%$, the investment lifespan $L = 20$ years, and replacement of the electrolyser stacks occurs after 10 years at the latest. The results of the analysis are presented in the following section.

3. Results

3.1. Effect of photovoltaics sizing on system performance

Before the presentation of the results regarding the LCOH, the effect of photovoltaic system sizing on various performance indicators of the plant is examined. The energy production and consumption profiles for $r = 1.67$ are illustrated in **Figure 5.a**. It appears that, for this specific power output profile, the effect of the electrolyser's slow response on its productivity is small, as the energy which is curtailed due to the cold start process is only a small fraction of that utilized toward hydrogen production.

Figure 5.b shows in detail the change in the distribution of the time the unit spends in each possible operating state as a function of r . The conclusion stated above is confirmed by the diagram, as the plant spends minimal time in transitional operating states (<3% of the year) regardless of the installed PV capacity. This is due to the nature of solar power generation (usually only one startup per day needed). The shape of the power output profiles also accounts for the unit remaining in off state for at least 50% of the year, since the PV system produces no power during nighttime hours. Of particular interest is the effect of PV sizing on the hours during which the unit remains in standby mode. For very low values of the r ratio (e.g., 0.25), the unit spends more time in standby mode than in operation. This occurs because the generated power is sufficient to meet standby operating conditions but insufficient for hydrogen production. As the value of r increases, the time during which there is sufficient power for hydrogen production increases, and thus the percentage of time during which the

electrolyser remains in standby diminishes at a decreasing rate. After a certain point, it becomes comparable to the corresponding (very low) percentage for startup procedures. For the same reason, an increase in r implies a decreasing-rate increase in the percentage of the year during which hydrogen is produced, which approaches a value close to 45%.

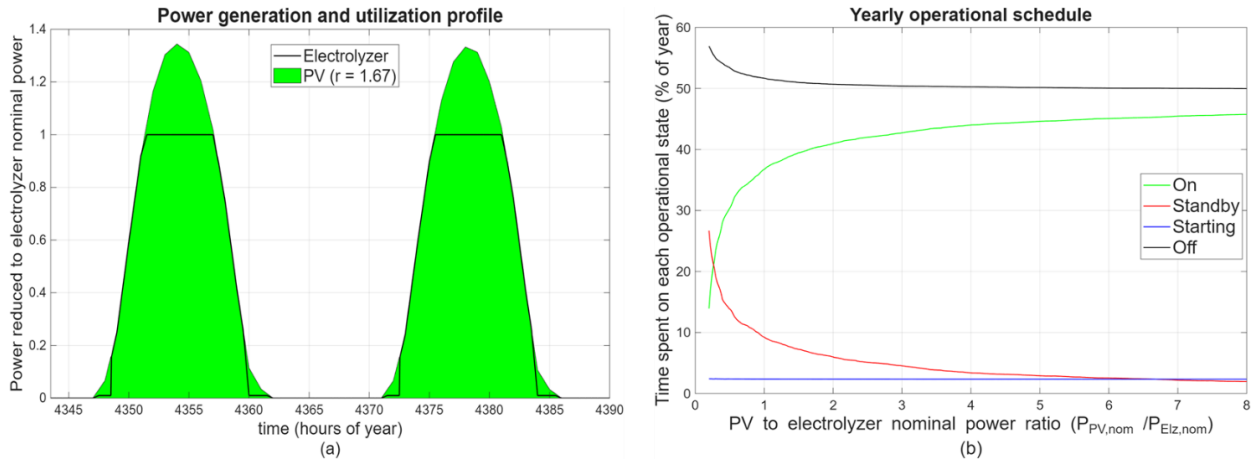


Figure 5: Power generation profile (a) and yearly operational schedule (b)

Figure 6 illustrates the impact of PV sizing on the annual amount of hydrogen produced and on the utilization of renewable energy. Specifically, the first graph shows the change in the annual amount of hydrogen produced, normalized to the nominal power of the electrolyser, at various stages of the electrolyser's life cycle. The difference in productivity from year to year is attributed to the degradation of the electrolyser, which is proportionate to the system's working hours at the on state. The electrolyser's degradation means that the same energy input results in less hydrogen being produced. It is observed that an increase in r results in a greater decline in productivity over the years. As noted above, higher power ratio values mean more operating hours and thus a greater drop in efficiency. Furthermore, the annual amount of hydrogen produced increases at a decreasing rate, similar to the operating hours at the on state.

The second diagram shows the distribution of PV energy utilization across the various operating states of the electrolyser, as a function of the power ratio r . A minimal portion of the PV energy generated is allocated to starting up and maintaining the unit in standby mode. This is due, on the one hand, to the low number of hours spent in these states and, on the other hand, to the comparatively low power required for these operating states. For very low values of r , the energy utilized for hydrogen production is comparable to curtailed energy. An increase in r leads to an increase in the percentage of energy utilized for hydrogen production and a decrease in the percentage of curtailed, as the number of hours during which there is sufficient power for production increases, without exceeding the electrolyser's rated capacity. The percentage of renewable energy available for production is maximized for $r \approx 1.1$. A further increase in r does not significantly alter the operating hours in the on state, while power surpluses become significantly higher. Thus, the percentage of curtailed energy increases again and eventually exceeds the percentage of energy utilized for hydrogen production.

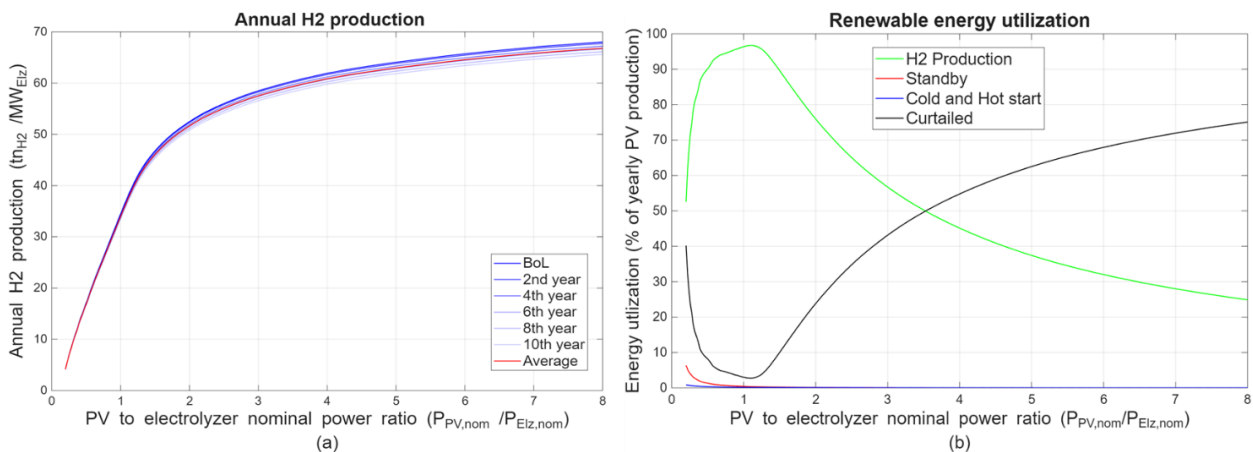


Figure 6: Annual H₂ production (a) and renewable energy utilization (b)

The aforementioned results have a significant impact on the system's economic performance. The variation in LCOH, as well as the electrolyser's capacity factor, is shown in **Figure 7**. Initially, the electrolyser's capacity factor increases in proportion to the annual hydrogen production. As far as the LCOH is concerned, it reaches very high values for $r \ll 1$. This is due to the very low $c_{F,elz}$, which indicates insufficient utilization of the electrolyser's capacity. An increase in r leads to a decrease in LCOH, which reaches a minimum value and then increases again, at a slower rate. This can be attributed to the fact that, beyond a certain point, the increase in production is small, with most of the additional energy being curtailed. Thus, costs rise disproportionately to the level of production, leading to inferior performance.

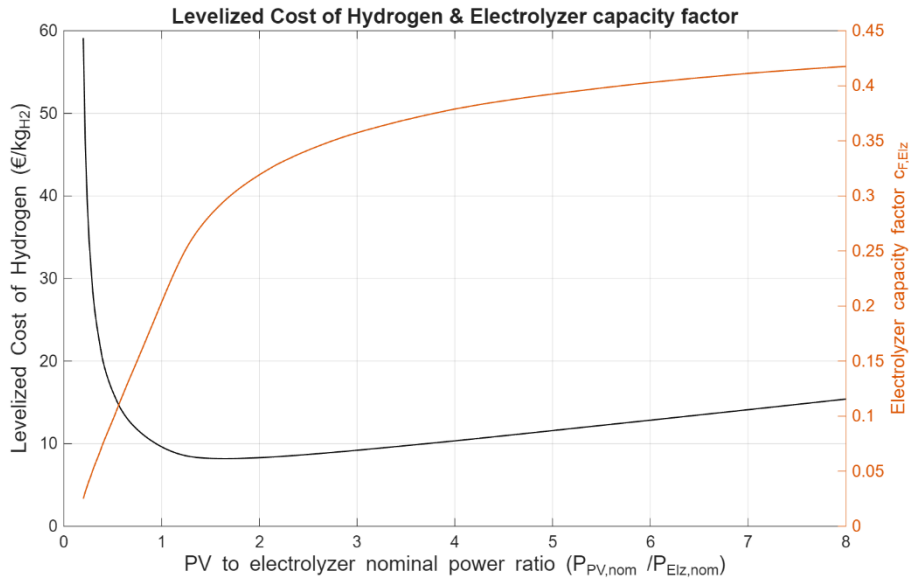


Figure 7: Levelized Cost of Hydrogen and electrolyzer capacity factor

Table 3 summarizes the characteristics of the optimal sizing and performance of the facility.

Table 3. System optimal sizing and performance

Parameter	Units	Value
Optimal power ratio r	-	1.67
Electrolyser capacity factor	%	30
Renewable energy utilization factor	%	85
Photovoltaics capacity factor	%	21
Average annual H_2 production	$(tn_{H_2}/MW_{elz})/year$	48.30
Levelized Cost of Hydrogen	$€/kg_{H_2}$	8.18

3.2. Effect of climate conditions on system optimal sizing and performance

The results presented above pertain to a specific region of Greece. Since the system's performance is directly linked to the level of photovoltaic production, production data were collected from 30 different locations around the world to determine the effect of climatic conditions on the optimal sizing and performance of the system. It should be noted that, to compare the LCOH for different countries, different assumptions regarding technology costs and the discount rate would normally need to be made, reflecting local conditions regarding investment risk and financing. However, the objective of the study is to investigate the impact of different climatic conditions on the characteristics of the installation, rather than to compare countries. For this reason, the initially – presented assumptions concerning the system's economic data are used.

Figure 8 illustrates the variation of the most important characteristics of the facility as functions of the photovoltaics' capacity factor. Greater emphasis is placed on the qualitative aspects of these variations rather than on the exact numerical values. The numerical results pertain only to the electrolyser for which the technical data have been collected. Initially, it appears that the optimal ratio r decreases as $c_{F,PV}$ increases (Figure 8(a)). This results in a reduction of the fraction of curtailed energy (Figure 8(d)), as a decrease in r also implies a reduction in production peaks during midday hours, which are the main cause of energy curtailment. Similarly, the average annual amount of hydrogen produced increases with an increase in $c_{F,PV}$, as better climatic conditions mean sunshine for a larger portion of the day and more operating hours at the rated point. The

analytical correlations linking the variables in Figures 8 (a), (b), and (d) are indicative of the general trend of the variations, but the quality of the fit to the simulation data suggests limited predictive capability.

Impact of PV capacity factor ($C_{F,PV}$) on system performance

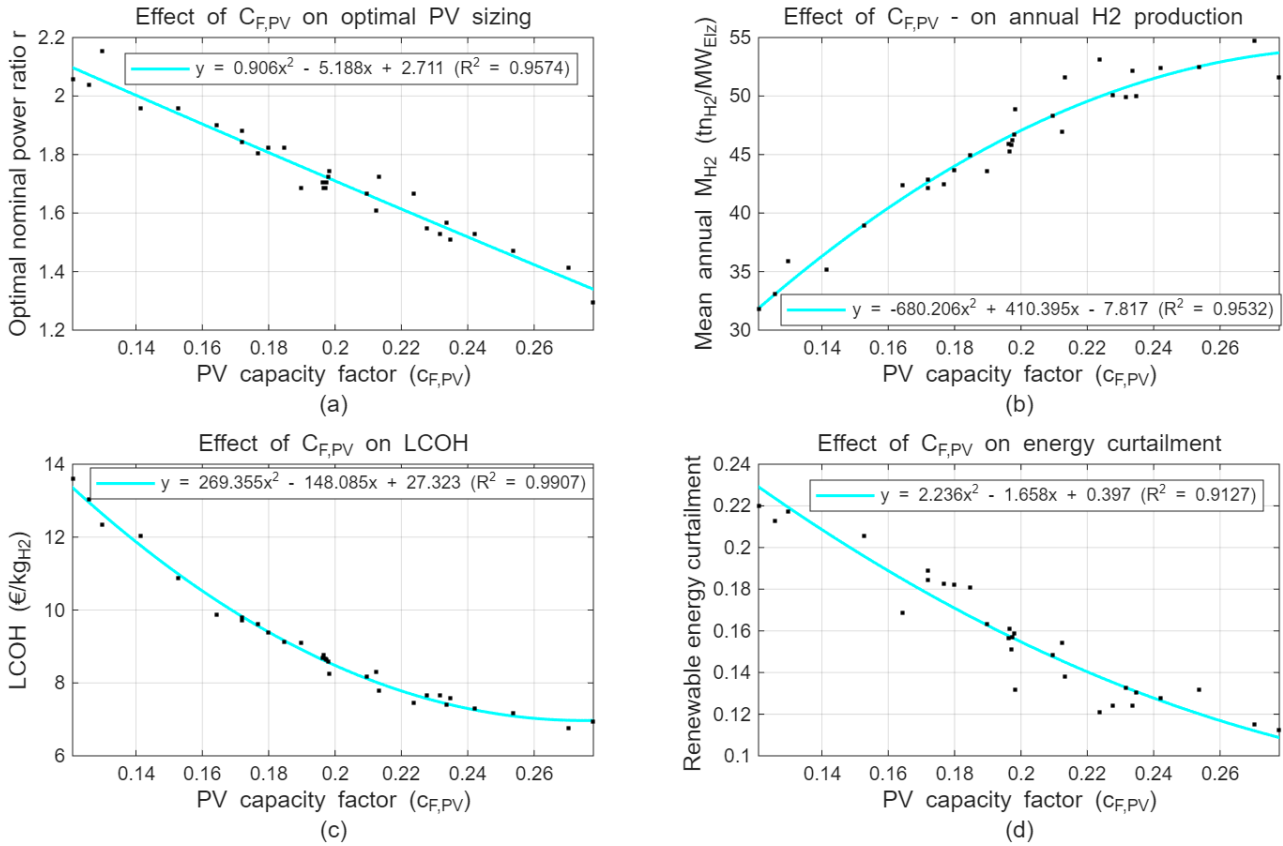


Figure 8: Impact of climate conditions on plant performance

In contrast, in the third graph, which shows the variation of LCOH as a function of the PV capacity factor, the regression function fits the simulation data exceptionally well. This is also confirmed by the values of the evaluation indices ($R^2 = 0.99, RMS < 2\%$). Therefore, the regression function can predict the system's economic performance with satisfactory accuracy under the current assumptions, without the need for simulation. The only data required is PV power production time series, from which the capacity factor of the photovoltaics is derived. It follows, therefore, that the LCOH decreases at a decreasing rate as $c_{F,PV}$ increases. This means that the economic viability of the plant is more affected by variations in climatic conditions in areas with lower solar radiation.

4. Conclusions and future work

The aim of this study was the development of a techno-economic evaluation and sizing optimization model of electrolysis systems coupled with photovoltaics. Regarding the design, under-sizing the PV system relative to the electrolyser leads to economically unsustainable results, primarily due to the underutilization of the electrolyser's capacity. On the other hand, oversizing the PV system makes no sense beyond a certain r value, as the amount of hydrogen produced increases only slightly and most of the excess renewable energy is curtailed. The optimal economic results for the case of Greece and the TRIERES electrolyser data correspond to $r = 1.67$ and $LCOH = 8.182 \text{ €/kg}_{H_2}$. Of particular interest is the fact that the optimal economic results do not imply a maximization of the degree of renewable energy utilization. Specifically, the optimal design results in $U_{PV} = 85.2\%$, while U_{PV} is maximized at $r \approx 1.1$, where $U_{PV} \approx 96.7\%$. It was also observed that climatic conditions significantly affect the economic performance of the installation, with the impact being more pronounced under low-sunlight conditions.

The results indicate that the electrolyser's capacity factor is quite low. Specifically, in the optimal design, $c_{F,elz} = 29.7\%$, while it does not exceed 45% even for very high values of r . Therefore, a worthy subject for

future study is the integration of energy storage systems into the model, with the aim of investigating the potential for better utilization of the electrolyser's capacity and increasing the amount of hydrogen produced.

Finally, it should be noted that power consumption during transient operating conditions was assumed to be constant, for the sake of simplicity. In reality, during transient conditions, power consumption increases gradually. As was ascertained above, the unit spends a minimal percentage of its time on startup procedures, and therefore the resulting error is negligible. However, for different generation profiles (e.g., from wind turbines rather than photovoltaics), where multiple startups may occur within a day, the error is expected to increase. Therefore, the way in which the electrolyser's power changes during startup warrants further investigation in the future.

Acknowledgement

The authors would like to acknowledge funding received within the framework of the TRIERES research project, funded by the Clean Hydrogen Partnership and its members Hydrogen Europe and Hydrogen Europe Research under Grant Agreement No. 101112056.

Nomenclature

Letter symbols

C	specific cost, €/kg
$CAPEX$	Investment cost, €
c_F	capacity factor
cs	operational state variable
cwc	cooling water cost, €
$degr$	degradation, h ⁻¹
dwc	demineralized water cost, €
E	energy, MWh
hs	operational state variable
i	interest rate
$LCOH$	Levelized Cost of Hydrogen, €/kg _{H2}
m	mass, kg
M	mass – annual production, kg
off	operational state variable
$OPEX$	plant operating cost, €
on	operational state variable
P	power, MW
r	PV to electrolyser nominal power ratio
$REPEX$	stack refurbishment cost, €
RY	stack refurbishment years
sb	operational state variable
U	utilization factor
\dot{V}	volumetric flow rate, m ³ /s
w	Electrolysis specific water consumption, kg _{H2O} /kg _{H2}

Greek symbols

Δt	time interval, s
η	electrolyser efficiency, kg _{H2} /MWh

Subscripts and superscripts

a	annual
CW	cooling water
cs	electrolyser state: stack heating
$curt$	curtailed

<i>DW</i>	demineralized water
<i>elz</i>	electrolyser
<i>j</i>	time step index
<i>h</i>	hourly
<i>hs</i>	electrolyser state: hot start
<i>min</i>	minimum
<i>nom</i>	nominal
<i>on</i>	electrolyser state: on
<i>PV</i>	photovoltaics
<i>sb</i>	electrolyser state: standby
<i>ts</i>	time step

References

- [1] A. Buttler, H. Spliethoff, Current status of water electrolysis for energy storage, grid balancing and sector coupling via power-to-gas and power-to-liquids: A review, *Renewable and Sustainable Energy Reviews* 82 (2018) 2440–2454. <https://doi.org/10.1016/J.RSER.2017.09.003>.
- [2] M. Nasser, T.F. Megahed, S. Ookawara, H. Hassan, A review of water electrolysis–based systems for hydrogen production using hybrid/solar/wind energy systems, *Environmental Science and Pollution Research* 29 (2022) 86994–87018. <https://doi.org/10.1007/s11356-022-23323-y>.
- [3] Delegated regulation - 2023/1185 - EN - EUR-Lex, (n.d.). <https://eur-lex.europa.eu/legal-content/EN/TXT/?uri=CELEX%3A32023R1185&qid=1704969410796> (accessed November 4, 2024).
- [4] J. Armijo, C. Philibert, Complying with low-emission hydrogen standards in long-term integrated supply chains, *Energy Policy* 198 (2025) 114504. <https://doi.org/10.1016/j.ijhydene.2019.11.028>.
- [5] T. Egeland-Eriksen, J.F. Jensen, Ø. Ulleberg, S. Sartori, Simulating offshore hydrogen production via PEM electrolysis using real power production data from a 2.3 MW floating offshore wind turbine, *Int. J. Hydrogen Energy* 48 (2023) 28712–28732. <https://doi.org/10.1016/J.IJHYDENE.2023.03.471>.
- [6] M.J. Ginsberg, D. V. Esposito, V.M. Fthenakis, Designing off-grid green hydrogen plants using dynamic polymer electrolyte membrane electrolyzers to minimize the hydrogen production cost, *Cell Rep. Phys. Sci.* 4 (2023) 101625. <https://doi.org/10.1016/J.XCRP.2023.101625>.
- [7] C. Moran, E. Moylan, J. Reardon, T.A. Gunawan, P. Deane, S. Yousefian, R.F.D. Monaghan, A flexible techno-economic analysis tool for regional hydrogen hubs – A case study for Ireland, *Int. J. Hydrogen Energy* 48 (2023) 28649–28667. <https://doi.org/10.1016/J.IJHYDENE.2023.04.100>.
- [8] F. Superchi, A. Mati, C. Carcasci, A. Bianchini, Techno-economic analysis of wind-powered green hydrogen production to facilitate the decarbonization of hard-to-abate sectors: A case study on steelmaking, *Appl. Energy* 342 (2023) 121198. <https://doi.org/10.1016/J.APENERGY.2023.121198>.
- [9] Clean Hydrogen JU - SRIA Key Performance Indicators (KPIs) - European Commission, (2021). https://www.clean-hydrogen.europa.eu/knowledge-management/strategy-map-and-key-performance-indicators/clean-hydrogen-ju-sria-key-performance-indicators-kpis_en (accessed April 9, 2024).
- [10] N. Skordoulias, S. Karellas, D. V. Lyridis, S.G. Giannissi, G. Mitkidis, RES-electrolyser coupling within TRIERES hydrogen valley – A flexible technoeconomic assessment tool, *Energy Convers. Manag.* 327 (2025) 119562. <https://doi.org/10.1016/J.ENCONMAN.2025.119562>.